The American Journal of Pathology, Vol. 184, No. 5, May 2014

The American Journal of
PATHOLOGY
ajp.amjpathol.org

CELL INJURY, REPAIR, AGING, AND APOPTOSIS

Inhibitory Effects of PPARγ Ligands on TGF-β1—Induced Corneal Myofibroblast Transformation

Kye-Im Jeon,* Ajit Kulkarni,† Collynn F. Woeller,‡ Richard P. Phipps,*†‡ Patricia J. Sime,†‡ Holly B. Hindman,*§ and Krystel R. Huxlin*§

From the Flaum Eye Institute, the Departments of Medicine† and Environmental Medicine,‡ and the Center for Visual Science,§ University of Rochester, Rochester, New York*

Accepted for publication January 16, 2014.

Address correspondence to Krystel R. Huxlin, Ph.D., Flaum Eye Institute, Box 314, University of Rochester Medical Center, 210 Crittenden Blvd., Rochester, NY 14642. E-mail: huxlin@cvs.rochester.edu.

Corneal scarring, whether caused by trauma, laser refractive surgery, or infection, remains a significant problem for humans. Certain ligands for peroxisome proliferator-activated receptor gamma (PPARγ) have shown promise as antiscarring agents in a variety of body tissues. In the cornea, their relative effectiveness and mechanisms of action are still poorly understood. Here, we contrasted the antifibrotic effects of three different PPARγ ligands (15-deoxy-Δ12,14-prostaglandin J2, troglitazone, and rosiglitazone) in cat corneal fibroblasts. Western blot analyses revealed that all three compounds reduced transforming growth factor (TGF)-β1—driven myofibroblast differentiation and up-regulation of α-smooth muscle actin, type I collagen, and fibronectin expression. Because these effects were independent of PPARγ, we ascertained whether they occurred by altering phosphorylation of Smads 2/3, p38 mitogen—activated protein kinase, stress-activated protein kinase, protein kinase B, extracellular signal-regulated kinase, and/or myosin light chain 2. Only p38 mitogen—activated protein kinase phosphorylation was significantly inhibited by all three PPARγ ligands. Finally, we tested the antifibrotic potential of troglitazone in a cat model of photorefractive keratectomy—induced corneal injury. Topical application of troglitazone significantly reduced α-smooth muscle actin expression and haze in the stromal ablation zone. Thus, the PPARγ ligands tested here showed great promise as antifibrotics, both *in vitro* and *in vivo*. Our results also provided new evidence for the signaling pathways that may underlie these antifibrotic actions in corneal fibroblasts. *(Am J Pathol 2014, 184: 1429—1445; http://dx.doi.org/10.1016/j.ajpath.2014.01.026)*

Maintaining the transparency and regular shape of the cornea are essential for normal vision. After corneal damage, stromal keratocytes that survive the injury become exposed to multiple wound healing mediators, including transforming growth factor (TGF)-β, the strongest known profibrotic agent.[1,2] As a result, corneal keratocytes proliferate, migrate, transform into fibroblasts,[3] and ultimately transform into myofibroblasts.[4] In some ways, myofibroblasts are well suited to restore corneal integrity after injury because they can contract wounds and secrete extracellular matrix components.[5] However, persistent myofibroblast activity also decreases corneal transparency,[6] and by contracting the cornea, they induce certain higher-order, optical aberrations, which negatively affect optical quality.[7]

TGF-β initiates profibrotic changes in cell behavior by binding TGF-β receptors on the cell surface, causing phosphorylation of several cytoplasmic substrates, including members of the Smad family. Smads 2 and 3 each form heterodimeric complexes with Smad 4, which translocates to the nucleus and activates transcription of select target genes.[8] However, TGF-β receptor binding also activates non-Smad intracellular signaling pathways, such as TGF-β—associated kinase 1, extracellular signal—regulated kinase (Erk), p38 mitogen—activated protein kinase (MAPK), Rho-associated protein kinase (ROCK), and

Supported by the NIH (grants EY015836, EY017123, HL75432, K23 EY019353, and core grant P30 EY001319 to the Center for Visual Science), an unrestricted grant to the Department of Ophthalmology (University of Rochester) from the Research to Prevent Blindness Foundation, and the Lew R. Wasserman Merit Award from the Research to Prevent Blindness Foundation (K.R.H.).

Disclosures: None declared.

http://dx.doi.org/10.1016/j.ajpath.2014.01.026

protein kinase B/AKT.[9] Because activation of TGF-β appears to be a central regulator of events during wound healing,[10] developing strategies to prevent TGF-β–related activities seems an appealing antiscarring approach. Confirming this notion, application of antibodies against TGF-β to the ocular surface reduced corneal reflectivity (haze) and fibrosis after photorefractive keratectomy (PRK) in rabbits[11] and cats.[7] However, epithelial healing was also slowed, and myofibroblast differentiation, stromal regrowth, haze, and increases in higher-order optical aberrations were not completely eliminated.[7,11]

Clinically, the most commonly used pharmacologic agents for the modulation of corneal wound healing after PRK in humans are mitomycin C[12] and steroids, such as prednisolone acetate.[13] Although short- and long-term adverse effects of mitomycin C have been reported,[12,14] long-term use of corticosteroids can depress immune reactions (predisposing individuals to infections), increase intraocular pressure (which can lead to permanent vision loss), and cause cataract formation (further disrupting optical clarity).[15] Thus, there is a need for better ways of treating corneal fibrosis, without the adverse effects inherent in mitomycin C or steroids and without the concern of applying anti–TGF-β antibodies to the eye.

In this context, our group and others have found several ligands of PPARγ to be effective corneal antifibrotics *in vitro*[16–18] and, most recently, *in vivo*.[19] PPARγ is a transcription factor belonging to a nuclear receptor superfamily that regulates important cellular functions, including metabolism, adipogenesis, proliferation, and differentiation, as well as inflammatory responses.[20] A significant body of mostly cell culture data suggests that PPARγ ligands can act as antifibrotics in several body tissues, including lung,[21] skin,[22] kidneys,[23] and cornea.[16–18] Interestingly, in cultured human corneal fibroblasts, the electrophilic ligands CDDO and 15-deoxy-Δ12,14-prostaglandin J2 (15d-PGJ2) appear to have stronger antifibrotic actions than nonelectrophilic ligands, such as rosiglitazone.[16] Yet, *in vivo*, rosiglitazone was highly effective at controlling corneal fibrosis after PRK in the cat eye, without any apparent adverse effects or toxicity.[19]

Our goal was to examine the antifibrotic properties of three different PPARγ ligands (troglitazone, rosiglitazone, and 15d-PGJ2) in cultured cat corneal fibroblasts. Understanding the mechanisms of action of different PPARγ ligands seems critical for estimating both their safety and efficacy in the context of corneal wound healing. Thus, we asked the following: i) what is the relative time course of expression of α-smooth muscle actin (α-SMA), collagen 1 (COL1), and fibronectin (FN) after TGF-β1 stimulation in cat corneal fibroblasts? ii) Are different classes of PPARγ ligands (electrophilic versus nonelectrophilic) equally effective as corneal antifibrotics *in vitro*? In particular, were prior reports of ineffectiveness of some nonelectrophilic ligands due to tissue, species differences, or suboptimal dosing? iii) When used at optimal doses, do all three PPARγ ligands decrease expression of α-SMA, COL1, and FN at the same rate and to the same extent? iv) What signaling pathways do PPARγ ligands influence in corneal fibroblasts, and are they important for mediating their observed antifibrotic effects?

Materials and Methods

All animal procedures were conducted according to the guidelines of the University of Rochester Committee on Animal Research, the Association for Research in Vision and Ophthalmology Statement for the Use of Animals in Ophthalmic and Vision Research, and the NIH Guide for the Care and Use of Laboratory Animals.

Isolation of Primary Cat Corneal Fibroblasts and Culture Conditions

Primary feline corneal fibroblasts were isolated from fresh, young, adult, domestic, short-hair cats (*Felis cattus*) by double collagenase digestion, as previously described.[19] Mitogen-poor horse serum (HS) was used here instead of fetal bovine serum (FBS) in an attempt to keep cells in a more quiescent state. Prior work has shown that cells cultured in HS retained their keratocyte morphologic features longer and secreted highly sulfated forms of keratin sulfate proteoglycan, a keratocyte marker.[3,24,25] In addition, Chen et al[26] confirmed that keratocan and CD34, both keratocyte markers, were expressed in bovine corneal cell cultured in Dulbecco's modified Eagle's medium (DMEM)/10% HS, whereas these molecules were not expressed in cells cultured in DMEM/10% FBS. Part of the reason why FBS might cause cultured cells to lose their keratocyte phenotype is that it contains high levels of latent TGF-β,[27] which can be activated by cell-associated plasmin[28] during the cell culture process. Passage 6 to 7 fibroblasts were used for all experiments and kept in 1% HS-DMEM/nutrient mixture F-12 (F12) for 1 day to promote cellular quiescence after attachment.

Immunocytochemistry

Corneal fibroblasts were seeded at a density of 1×10^4 cell/well in Lab-Tek II Chamber slides in 5% HS-DMEM/F12. Cells were then pretreated with optimal doses of the three PPARγ ligands (15 μmol/L troglitazone, 75 μmol/L rosiglitazone, and 5 μmol/L 15d-PGJ2) in 1% HS-DMEM/F12 for 30 minutes. TGF-β1 (1 ng/mL) was then added to the medium, and the cells were incubated for 3 days without any medium changes. For immunofluorescent staining, the chamber slides were rinsed with DMEM/F12 without serum and fixed with 4% paraformaldehyde (Electron Microscopy Sciences, Hatfield, PA) in 1× PBS on ice for 15 minutes, followed by permeabilization with acetone (J. T. Baker, New York, NY) at −20°C for 10 minutes. Nonspecific binding was blocked with 3% normal goat serum (Jackson

ImmunoResearch, West Grove, PA) and 0.025% Triton X-100 (Sigma-Aldrich, St. Louis, MO) in 1× PBS for 30 minutes. Primary antibodies were then applied to the slides. They included polyclonal rabbit anti-mouse FN (1:150, AB2033, Millipore, Billerica, MA) and monoclonal mouse anti-human α-SMA (1:400, clone 1A4, ThermoScientific, Waltham, MA). The slides were incubated at 4°C overnight. After washing off the primary antibodies with 1× PBS, the slides were incubated with secondary goat anti-rabbit IgG conjugated to Alexa Fluor 488 (1:500, A11008, Invitrogen, Carlsbad, CA) and goat anti-mouse IgG conjugated to Alexa Fluor 555 (1:300, A21422, Invitrogen) for 2 hours at room temperature. Slides were coverslipped using Vectashield plus DAPI (Vector Laboratories, Burlingame, CA). Finally, the triple-labeled cell cultures were imaged using an Olympus AX70 fluorescence microscope, and photomicrographs were collected via a high-resolution video camera interfaced with a personal computer running the ImagePro software (MediaCybernetics, Bethesda, MD).

Effect of PPARγ Ligands on TGF-β1–Induced Expression of α-SMA, COL1, and FN in Cultured Corneal Fibroblasts

A density of 2.5×10^4 to 7.5×10^4 cells/well in 6-well plates was used. The cells were then pretreated with each of the three PPARγ ligands of interest [troglitazone (Cayman Chemical Company, Ann Arbor, MI), rosiglitazone (Cayman Chemical Company), or 15d-PGJ2 (Enzo, Plymouth Meeting, PA)] in 1% HS-DMEM/F12 medium (rather than serum-free medium) for 30 minutes to avoid cytotoxicity on addition of 15d-PGJ2. One nanogram per milliliter of recombinant human TGF-β1 (R&D Systems Inc., Minneapolis, MN) was then added to the medium, and the cells were incubated for 1, 2, or 3 days without any medium changes. Western blot analysis was then performed as previously described.[19]

PPARγ Dependency of Antifibrotic Effects in Cultured Corneal Fibroblasts

To test whether the observed antifibrotic effects of troglitazone, rosiglitazone, and 15d-PGJ2 were PPARγ dependent or independent, we used both a pharmacologic and a genetic approach that blocked PPARγ function in our cultured corneal fibroblasts. For the pharmacologic approach, cat corneal fibroblasts were seeded and kept quiescent for 1 day as described above. Cells were then pretreated with 0.5 or 1 μmol/L of the synthetic PPARγ antagonist GW9662 (Cayman Chemical Company) for 1 hour, after which optimal doses of PPARγ ligands were added for 30 minutes before the addition of TGF-β to the medium. The cells were incubated for 3 days before harvesting and evaluation by Western blot analysis.

To verify the effectiveness of GW9662 (as well as of the genetic approach described below) at blocking PPARγ function in cat cells, we ran a separate, control experiment in which cat orbital fibroblasts were isolated. This class of cells is closely related to corneal keratocytes but is able to synthesize fat in a PPARγ-dependent manner.[29] Approximately 500 to 1000 mg of feline orbital fat was rinsed three times in PBS and cut into approximately 2- to 4-mm^3 pieces. Samples were then digested in 5 mL of HBSS containing collagenase (200 U/mL) for 90 minutes at 37°C, mixing every 10 minutes. The reaction was stopped with the addition of DMEM/10% FBS, and cells were collected by centrifugation (1000 × *g* for 10 minutes). They were then plated and cultured in DMEM/10% FBS in 10-cm^2 dishes to establish fibroblast strains. After culture expansion, passage 4 orbital fibroblasts (5000 cells/cm^2) were plated in 24-well plates (Corning, Corning, NY) and grown in DMEM/5% FBS to confluence. The medium was then replaced with vehicle [dimethylsulfoxide (DMSO)] or 5 μmol/L 15d-PGJ2 (Cayman Chemical Company) and 1 μg/mL of insulin (Sigma-Aldrich) to stimulate adipogenesis according to standard protocols.[30] A fraction of the wells also received 1 μmol/L GW9662 alone. The culture medium was replaced every 2 days for a total of 8 days of treatment. To wells receiving GW9662, 1 μmol/L fresh GW9662 was added every day of the experiment. On the eighth day, adipogenesis was measured using the AdipoRed reagent (Cayman Chemical Company), which measures neutral lipid accumulation inside the cells. Briefly, culture medium was aspirated and samples were rinsed in room temperature PBS. Samples were incubated with the AdipoRed reagent for 10 minutes at room temperature in the dark to allow for lipid-AdipoRed binding. The plates were then excited at 485 nm in a Varioskan Flash Multimode Reader (ThermoScientific), and fluorescence was quantified at 572 nm.

Lentiviral (Lv) transduction of a dominant negative (DN) PPARγ construct was used as a second method to test whether PPARγ ligands function in a PPARγ-independent manner. Green fluorescent protein (GFP)-Lv and PPARγ-DN-Lv (which encoded flag-tagged PPARγ1 L466A/E469A) were produced as previously described.[31] Feline corneal fibroblasts or feline orbital fibroblasts were plated as above and infected with GFP-Lv or PPARγ-DN-Lv at a multiplicity of infection of 10 for 24 hours. The medium was replaced and infected cells were treated as above to test PPARγ dependency in corneal fibroblasts with PPARγ ligands and TGF-β treatment and in orbital fibroblasts with adipogenic treatment. Myofibroblast formation and adipogenesis were measured by Western blot analysis and the Adipored assay, respectively, as described above.

Effect of PPARγ Ligands on TGF-β1–Induced Phosphorylation of Smads 2/3 in Cultured Corneal Fibroblasts

To study whether PPARγ ligands used in the present experiments affected phosphorylation of Smads 2/3, corneal fibroblasts were seeded and incubated under a low-serum condition as mentioned earlier. Pretreatment with PPARγ

ligands for 30 minutes was followed by addition of 1 ng/mL of TGF-β1 to the medium. Cells were incubated for 1 to 6 hours before sampling for Western blot analysis. The primary antibodies used in these Western blots included antiphosphorylated Smad 2 (Ser465/467; Millipore), anti-phosphorylated Smad 3 (Ser423/425; Millipore), and total anti-Smads 2/3 (D7G7; Cell Signaling, Beverly, MA).

Effect of PPARγ Ligands on TGF-β1–Induced Nuclear Translocation of Smads 2/3 in Cultured Corneal Fibroblasts

After TGF-β1 stimulation, phosphorylated Smads 2/3 form complexes with Smad 4 and translocate to the nucleus, where they regulate transcription of target genes.[32] After assessing the effect of PPARγ ligands on phosphorylation of Smads 2/3, it was also important to assess whether PPARγ ligands affected the translocation of p-Smads 2/3 into the nucleus. Thus, 1.5×10^6 cells per 10-cm dishes were pretreated with 15 μmol/L troglitazone. Cells were then treated with TGF-β1 for 1 hour before being washed with 1× Dulbecco's PBS containing 1 mmol/L sodium orthovanadate (NO_3VO_4; Sigma-Aldrich). We then added 1 mL of Trypsin-EDTA (0.25%; Gibco BRL, Gaithersburg, MD) and collected and centrifuged at 400 × *g* for 5 minutes; the pellet was then rinsed once or twice in ice-cold 1× Dulbecco's PBS containing 1 mmol/L NO_3VO_4. The pellet was gently resuspended in 200 μL of lysis buffer B (10 mmol/L Tris, pH 8.4, 140 mmol/L NaCl, 1.5 mmol/L $MgCl_2$, 1 mmol/L dithiothreitol, 0.1% NP-40, 0.5 mmol/L phenylmethylsulfonyl fluoride, 1 mmol/L NO_3VO_4, and complete protease inhibitor) without 0.1% NP-40. Cellular morphology was checked under a microscope to verify that the cells were rounding up without aggregating, at which stage 0.05% NP-40 was added while slowly vortexing for 10 to 15 seconds. More than 90% of cells ruptured as a result. The broken cell suspension was incubated on ice for 5 minutes before lysates were pelleted by centrifugation at 15,350 × *g* for 20 seconds at 4°C. After centrifugation, the supernatant was saved as the cytoplasmic fraction. The pellet fractions were rinsed once in lysis buffer B. Regular cell lysis buffer was then added and kept on ice for 10 minutes. Finally, the lysates were centrifuged at 15,350 × *g* for 10 minutes, and the supernatants were now saved as the nuclear fractions. To check for cross-contamination between cytoplasmic and nuclear fractions, anti–β-tubulin was used as a cytoplasmic marker, and purified mouse anti-SC35 (BD Pharmingen, San Jose, CA) was used as a nuclear marker.

Effect of TGF-β1 Stimulation on Phosphorylation of Downstream Signaling Molecules in Cat Corneal Fibroblasts

To assess the involvement of different non-Smad intracellular signaling pathways in TGF-β–induced responses, fibroblasts were cultured as described for the phosphorylated Smads 2/3 experiment. Cells were treated with 1 ng/mL of TGF-β1 and incubated for times ranging from 10 minutes to 24 hours before sampling to run Western blots. The antibodies for candidate kinases tested included anti-phosphorylated p38 MAPK (Thr180/Tyr182), anti-phosphorylated Akt (Ser473), anti-phosphorylated p44/42 MAPK (Erk1/2; Thr202/Tyr204), anti-phosphorylated SAPK/JNK (Thr183/Tyr185), and anti-phosphorylated MLC2 (Thr18/Ser19). All antibodies were purchased from Cell Signaling Technology. We evaluated the expression of phosphorylated p38 relative to total levels of p38 and of phosphorylated JNK, phosphorylated Akt, phosphorylated ERK, and phosphorylated MLC2 relative to β-tubulin via densitometric measurements.

Effect of Kinase Inhibitors on TGF-β1–Induced Expression of α-SMA, COL1, and FN in Cultured Corneal Fibroblasts

Our next goal was to identify the intracellular pathways most strongly activated by TGF-β1 stimulation in cat corneal fibroblasts under our particular cell culture conditions. We therefore used several small-molecule kinase inhibitors to block the major, known, endogenous, profibrotic protein kinases[9] and monitored the resultant molecular changes. Specifically, we used a TGF-β receptor 1 inhibitor (SB431542),[33] a Rho-associated kinase (Rho-kinase) inhibitor (H-1152),[34] an ERK inhibitor (U0126),[35] a JNK inhibitor (JNK inhibitor III and SP600125),[36] a p38 MAPK inhibitor (SB203580),[37] and an AKT inhibitor (LY294002).[38] All inhibitors were obtained from Calbiochem (San Diego, CA). Fibroblasts were seeded at a density of 1×10^5 cells/well in 6-well plates according to protocols outlined above. Dose dependence for each kinase inhibitor was first determined by pretreating cells in DMEM/F12/1% HS for 30 minutes, after which 1 ng/mL of TGF-β1 was added to the medium, and the cells were incubated for 3 days. Western blots were performed to assess the expression of α-SMA, COL1, and FN as described earlier.

Effect of PPARγ Ligands on TGF-β1–Induced p38 MAPK Signaling in Cultured Corneal Fibroblasts

To assess whether the p38 MAPK signaling pathway might be a specific target of our three PPARγ ligands of interest, fibroblasts were seeded at a density of 2.5×10^4 to 7.5×10^4 cells per well in 6-well plates and treated as described earlier. The cells were incubated for 2 days without any medium changes. The expression of phosphorylated p38 MAPK relative to total levels of p38 was then evaluated.

Antifibrotic Effects of Troglitazone *in Vivo*

To assess whether PPARγ ligands could inhibit corneal fibrosis *in vivo,* as well as *in vitro*, we used PRK to induce identical corneal wounds in the eyes of adult, domestic, short-hair cats, using well-established protocols.[39] In brief, a

−10D, conventional PRK was performed over a 6-mm optical zone with a central ablation depth of 168 μm (Planoscan 4.14; Bausch & Lomb, Rochester, NY). All procedures were performed under topical (0.5% proparacaine; Falcon, Fort Worth, TX) and surgical anesthesia (5 $mg \cdot kg^{-1}$ ketamine, 0.04 $mg \cdot kg^{-1}$ medetomidine hydrochloride), using a Technolas 217 laser (Bausch & Lomb). Immediately after PRK, drugs were applied to each eye and held in place on the stromal bed using a saturated, sterile, gelatin sponge (Surgifoam; Ethicon, Piscataway, NJ) for 2 minutes. Each eye then received a drop of antibiotic solution (neomycin, polymyxin B sulfate, gramicidin ophthalmic solution USP; Bausch & Lomb).

A first group of three animals was used to establish the optimal dose of troglitazone for this application. For the following 2 weeks, one eye of each cat received 1 drop (50 μL) of troglitazone (Cayman Chemical Company) diluted in vehicle solution consisting of 10% DMSO in Celluvisc (RefreshCelluvisc; Allergan, Irvine, CA) twice per day and one drop of antibiotic daily, whereas the other eye received vehicle solution (10% DMSO in Celluvisc) followed by one drop of antibiotic daily. Three different concentrations of troglitazone were tested: 1 μmol/L, 10 μmol/L, and 100 μmol/L. Cats were monitored for the development of haze via direct observation and once per week via OCT imaging, as previously described.[39,40] In brief, OCT imaging sessions required that the animals receive general anesthesia, as for PRK. Lubricating gel (GenTeal; Novartis, East Hanover, NJ) was applied to each eye. The head was stabilized, and the OCT was centered on the pupil. Videos of the central 10 mm of each cornea were collected at eight frames per second.

Once the optimal dose of troglitazone application *in vivo* was identified (10 μmol/L), an additional nine cats underwent identical, bilateral PRK to assess the optical and histologic effect of troglitazone treatment in a larger cohort and for a longer period (12 weeks postoperatively). PRK procedures and postoperative drug administration were as described above, except that 10 μmol/L troglitazone was the only dose of this drug used. Troglitazone was administered to one eye of each cat, whereas the other eye received vehicle for 2 weeks after PRK. OCT imaging was performed preoperatively, then every 2 weeks after PRK for 12 weeks. Measurement of backscatter reflectivity, which can be used as an index of haze in the anterior cornea, was performed as follows: four sampling lines were drawn in each of 10 corneal images per eye per time point. Of the four sampling lines, two were on each side of the central pixel of each image, starting approximately 1 mm from the corneal center, and with each pair of lines further separated by approximately 1 mm. A pixel intensity profile from epithelium to endothelium was generated for each line in ImageJ version 64 (National Institutes of Health, Bethesda, MD) before averaging across all four lines. To compensate for fluctuations in laser strength, mean profiles were normalized to the mean pixel intensity in a background region (exterior to the cornea) in each image. The region of the curve corresponding to the stroma was then divided into thirds, and we computed the mean, normalized pixel intensity over the anterior and posterior thirds in each image. These pixel intensity values were then averaged across 10 images per eye per time point.

At 2 and 4 weeks after PRK (and 2 weeks after stopping administration of troglitazone or vehicle to the eyes), four cats were euthanized so that the corneas could be excised and processed for histologic analysis. Excised corneas were drop-fixed in 1% paraformaldehyde/0.1 mol/L PBS, pH 7.4, for 10 minutes. They were then transferred to 30% sucrose/0.1 mol/L PBS and stored at 4°C for 2 days. After embedding into blocks (Tissue Tek O.C.T. Compound; Sakura Finetek, Zoeterwoude, Netherlands), serial cross sections (20 μm thick) were cut on a cryostat (2800 Frigocut E; Leica, Nußloch, Germany), mounted on microscope slides, and stored in a −20°C freezer until ready to stain. Slides containing three corneal sections each were air dried and rinsed in 0.01 mol/L PBS. Two sections per slide were incubated overnight at 4°C with 2 $\mu g \cdot mL^{-1}$ mouse monoclonal anti−α-SMA antibody (clone 1A4; Sigma-Aldrich). The third section was incubated with 0.1 mol/L PBS as a negative control. After washing off the primary antibody with 0.01 mol/L PBS, sections were reacted with anti-mouse IgG tagged with AlexaFluor 488 (2 $\mu g \cdot mL^{-1}$; Molecular Probes, Eugene, OR), followed by 0.1 $\mu g \cdot mL^{-1}$ propidium iodide (Invitrogen) to label cell nuclei. Double-labeled sections were imaged using an Olympus AX70 fluorescence microscope, and photomicrographs were collected via a high-resolution video camera interfaced with a personal computer running ImagePro software version 5.0 (MediaCybernetics).

Statistical Analysis

When three or more groups were compared, intergroup differences were tested with either a two-way analysis of variance or a one-way analysis of variance as applicable. When only two groups were compared, a two-sided Student's *t*-test was performed. A probability of error of $P < 0.05$ was considered statistically significant unless a Bonferroni correction was applied for multiple comparisons, in which case significant *P* values were indicated in the text. All statistical tests were performed using the SPSS software package version 20.0.0 (SPSS Inc., Chicago, IL).

Results

PPARγ Ligands Decrease TGF-β1–Induced Expression of α-SMA, COL1, and FN

In the absence of TGF-β1 stimulation, basal levels of α-SMA expression were close to zero in cat corneal fibroblasts, whether at 1, 2, or 3 days in culture (Figures 1, 2 and 3). However, the basal levels of COL1 and FN were distinctly above zero, confirming that these two extracellular matrix components were constitutively synthesized at low levels by corneal fibroblasts *in vitro*.

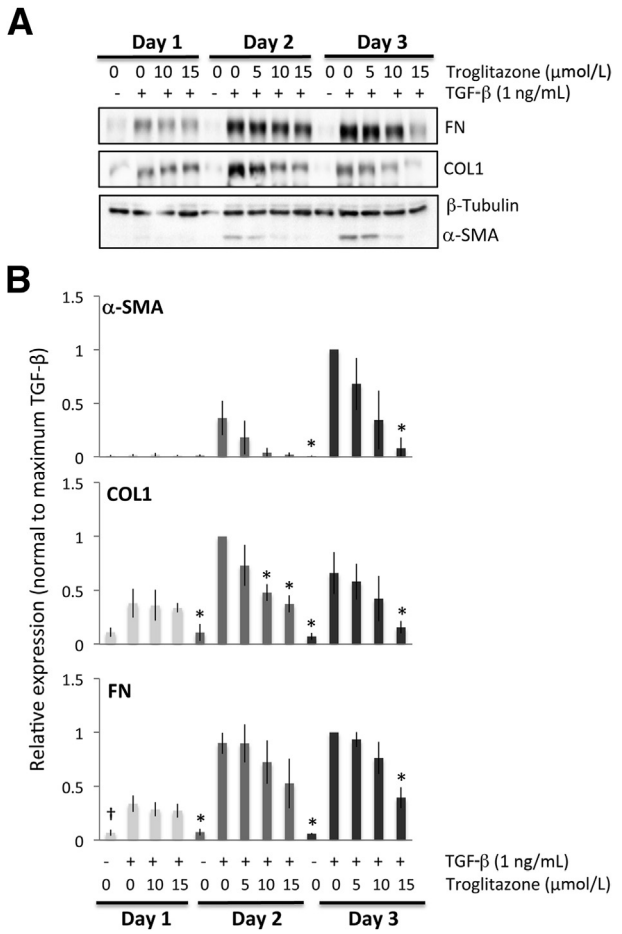

Figure 1 Antifibrotic effects of troglitazone on feline corneal fibroblasts. **A:** Representative Western blots show protein levels for fibronectin (FN), collagen type I (COL1), and α-SMA, with β-tubulin levels assayed as a loading control. β-tubulin levels were stable throughout. **B:** Plots of relative expression of FN, COL1, and α-SMA normalized to densitometric values obtained in cells stimulated with only 1 ng/mL TGF-β1 for each culture day sampled. Data are means ± SD averaged for three experiments. $^{*}P < 0.0125$ (four comparisons), $^{\dagger}P < 0.0167$ (three comparisons) by Bonferroni-corrected Student's *t*-test relative to TGF-β1–only condition ($df = 4$ for all tests).

After 1 day of culture (Figure 1A), troglitazone appeared to have no effect on the expression of FN and COL1, whereas α-SMA expression did not sufficiently increase to assay any inhibitory effects. After 2 days in culture, troglitazone still exerted no significant effect on α-SMA or FN expression, but it exerted a significant dampening of COL1 expression at the two highest doses of 10 μmol/L and 15 μmol/L. After 3 days of culture, 15 μmol/L of troglitazone administered together with TGF-β clearly inhibited the expression of all three profibrotic proteins relative to levels expressed after incubation with TGF-β alone for 3 days (Figure 1B).

Although some effect could be observed at lower doses, rosiglitazone clearly inhibited the expression of all three TGF-β1–induced profibrotic proteins at 75 μmol/L, whereas β-tubulin levels remained stable (Figure 2A). After 1 day of culture, rosiglitazone appeared to have no statistically significant effect on the expression of COL1, whereas α-SMA expression did not sufficiently increase at this time point to assay the effect of rosiglitazone. Only FN expression was significantly decreased by 75 μmol/L rosiglitazone. After 2 days in culture, 75 μmol/L rosiglitazone significantly decreased expression of α-SMA and COL1 relative to the TGF-β–only conditions. After 3 days of culture with 75 μmol/L of rosiglitazone and TGF-β, expression of α-SMA and FN decreased significantly relative to the TGF-β–only condition (Figure 2B).

After 1 day of culture, 15d-PGJ2 had a statistically significant effect on the expression of COL1 and FN, whereas α-SMA expression did not sufficiently increase at this time point to assess any inhibitory effects. After 2 and 3 days in culture, the quantitative analysis confirmed that all doses used significantly and completely prevented the induction of α-SMA expression. However, for COL1 and FN only the highest dose of 15d-PGJ2 (5 μmol/L) was able to significantly decrease protein expression relative to the TGF-β–only condition (Figure 3, A and B).

In summary, after 1 day of treatment with TGF-β1, α-SMA, COL1, and FN levels increased by four- to fivefold relative to vehicle-treated control cultures (Figure 4A). After 2 and 3 days of treatment with TGF-β1, although the expression of all three molecules increased even higher relative to the vehicle-treated condition, the effect of TGF-β on α-SMA appeared greater than on COL1 and FN (Figure 4A), with means ± SEM Western blot band intensities for α-SMA of 23 ± 2.6-fold and a 60- ± 13.3-fold increase relative to baseline at 2 and 3 days in culture, respectively. In contrast, COL1 levels increased by means ± SEM of 14 ± 3.7-fold and 11 ± 2.7-fold respectively, and FN levels increased by 12 ± 1.9-fold and 25 ± 6.0-fold, respectively after 2 and 3 days in culture. An analysis of variance probing the effect of incubation time with TGF-β (1, 2, or 3 days) on fold change in the expression of the three molecules of interest relative to their vehicle-treated levels revealed a significant effect of time, with the effect being strongest for α-SMA expression ($F_{2,23} = 12.946$, $P < 0.0005$), followed by FN expression ($F_{2,23} = 7.095$, $P = 0.004$) and weakest for COL1 ($F_{2,23} = 3.676$, $P = 0.041$). Thus, with respect to intracellular expression of α-SMA, COL1, and FN, we observed differences in the magnitude and, especially for COL1, in the duration of induction in cat corneal fibroblasts after stimulation with TGF-β1 under our culture conditions (Figure 4, A–D).

All three PPARγ ligands significantly decreased TGF-β1–induced expression of α-SMA, COL1, and FN at all time points examined. However, because a larger induction of these three molecules was obtained in corneal fibroblasts after 2 to 3 days of stimulation with TGF-β1, the effect of the PPARγ ligands was much clearer at these later time points (Figures 1, 2, 3, and 4). Furthermore, as shown in Figures 1, 2, and 3, the inhibitory effects of the three PPARγ ligands tested were clearly dose dependent, and when normalized to the maximal levels of α-SMA, COL1, and FN induced by TGF-β, the three compounds also showed some interesting differences in the effect on α-SMA versus COL1 and FN

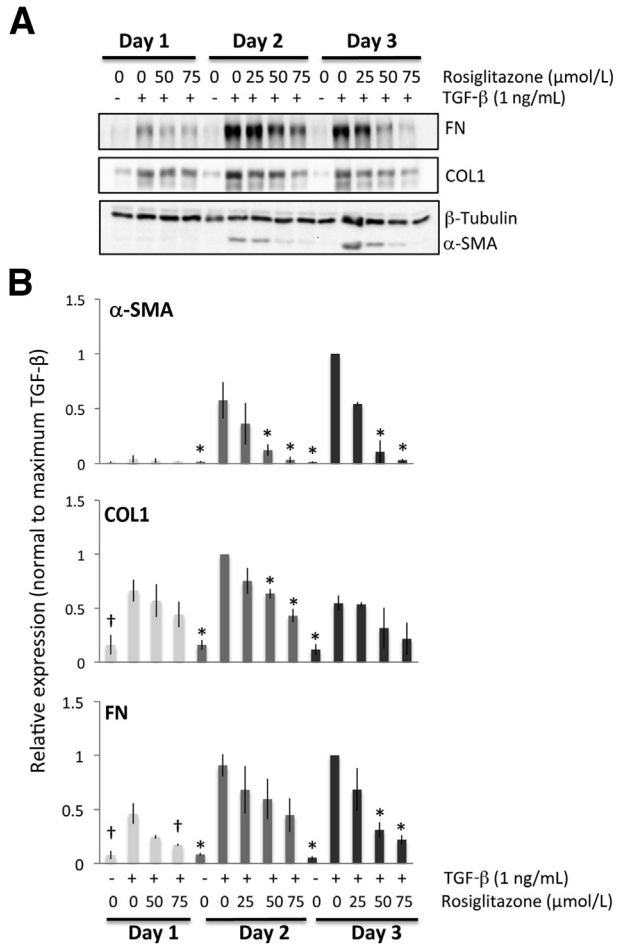

Figure 2 Antifibrotic effects of rosiglitazone on feline corneal fibroblasts. **A:** Representative Western blots showing protein levels for fibronectin (FN), collagen 1 (COL1), and α-SMA. β-tubulin was used as a loading control. **B:** Plots of relative expression of FN, COL1, and α-SMA normalized to densitometric values obtained in cells stimulated with 1 ng/mL of TGF-β1 for each culture day sampled. Data are means ± SD averaged for three experiments. $^{*}P < 0.0125$ (four comparisons), $^{\dagger}P < 0.0167$ (three comparisons) by Bonferroni-corrected Student's *t*-test relative to the TGF-β1–only condition ($df = 4$ for all tests).

expression (Figure 4, B–E). We performed an analysis of variance probing the effect of treatment (with the three different PPARγ ligands) on fold change in the expression of the three molecules of interest relative to their vehicle-treated levels to ascertain whether optimal doses of the three PPARγ ligands exerted essentially identical effects on these three molecules of interest. For COL1 ($F_{2,6} = 0.103$, $P = 0.904$) and FN ($F_{2,6} = 1.776$, $P = 0.248$), the three ligands behaved similarly, but in the case of α-SMA, there were significant differences in the different ligands' abilities to inhibit α-SMA expression ($F_{2,6} = 9.248$, $P = 0.015$).

As mentioned earlier, different ligands were most effective at different doses. With respect to TGF-β1–induced α-SMA expression, after 2 days in culture, the lowest effective doses were 15 μmol/L for troglitazone, 50 μmol/L for rosiglitazone, and 1 μmol/L for 15d-PGJ2, which was sufficient to significantly knock down α-SMA expression (5 μmol/L was the highest nontoxic dose). Similar results were obtained after 3 days in culture. Basically, the electrophilic PPARγ ligand 15d-PGJ2 could decrease TGF-β1–induced α-SMA expression at much lower doses (10- to 75-fold lower) than either of the two thiazolidinediones.

However, even when used at the right dose, troglitazone and 15d-PGJ2 were able to decrease α-SMA levels back to baseline levels of expression (0.8 ± 0.2-fold above baseline compared with 60 ± 11-fold above baseline when incubated with just TGF-β1 for 3 days). This represented an approximately 60-fold reduction in TGF-β1–induced α-SMA expression as a result of treatment with these PPARγ ligands. In contrast, rosiglitazone decreased α-SMA levels to only 2 ± 0.3-fold above baseline, still a 30-fold reduction relative to the TGF-β1–stimulated condition but nevertheless a significantly lesser effect than that exerted by troglitazone ($P = 0.048$, $df = 4$) and 15d-PGJ2 ($P = 0.019$, $df = 4$).

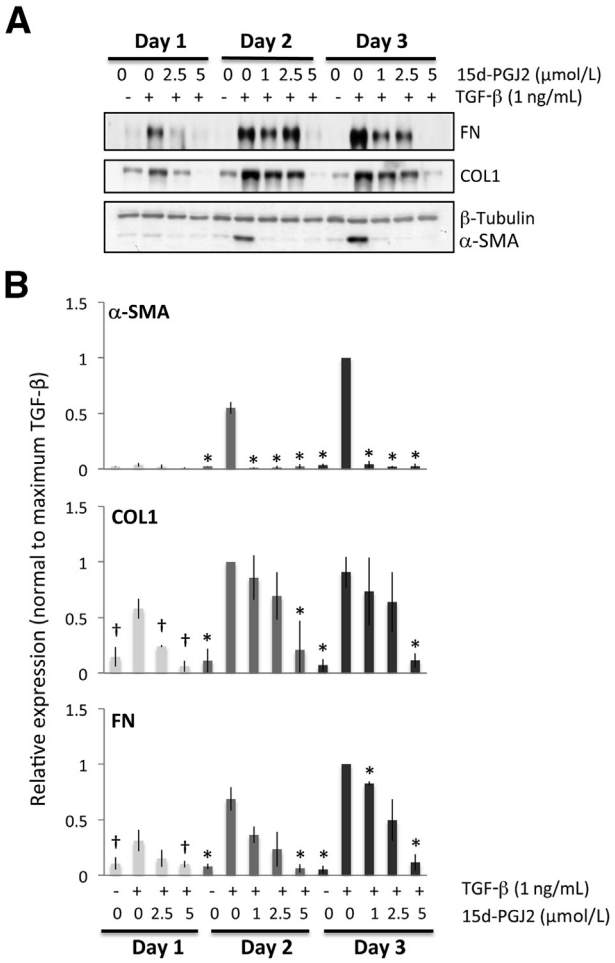

Figure 3 Antifibrotic effects of 15d-PGJ2 on feline corneal fibroblasts. **A:** Representative Western blots showing protein levels for fibronectin (FN), collagen 1 (COL1), and α-SMA. β-tubulin levels were assayed as a loading control. **B:** Plots of relative expression of FN, COL1, and α-SMA normalized to maximum densitometric values obtained in cells stimulated with 1 ng/mL of TGF-β1 for each culture day sampled. Data are means ± SD averaged for three experiments. $^{*}P < 0.0125$ (four comparisons), $^{\dagger}P < 0.0167$ by Bonferroni-corrected Student's *t*-test relative to the TGF-β–only condition ($df = 4$ for all tests).

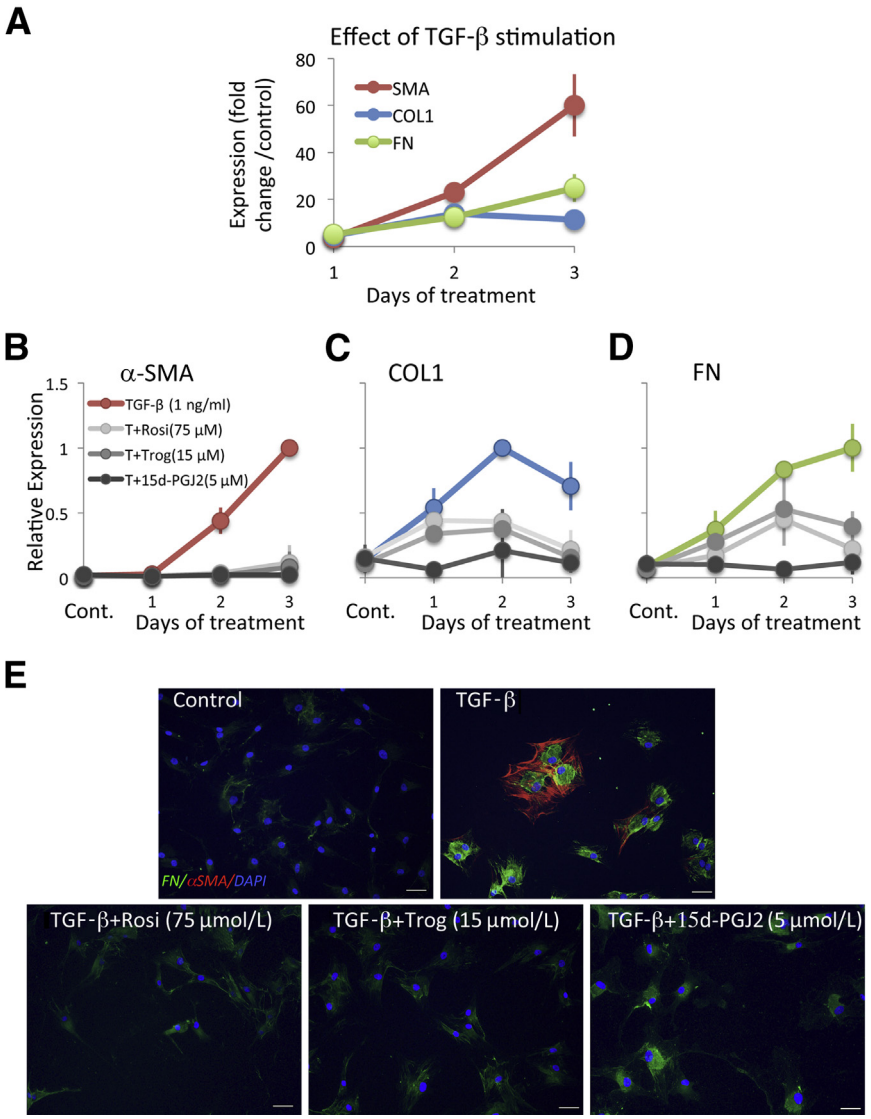

Figure 4 Comparative effect of TGF-β and PPARγ ligands on expression of α-SMA, collagen 1 (COL1), and fibronectin (FN) in feline corneal fibroblasts. **A:** Plot of change in expression of α-SMA, COL1, and FN induced by TGF-β1 in cultured cat corneal fibroblasts for 1, 2, or 3 days in culture relative to the control (vehicle-treated) condition. **B**—**D:** Plots of the effect of the optimal doses of the three PPARγ ligands of interest on expression of TGF-β1—induced α-SMA (**B**), TGF-β1—induced COL1 (**C**), and TGF-β1—induced FN (**D**). Changes in expression due to TGF-β alone (red in **B**, blue in **C**, and green in **D**). **E:** Cultured cat corneal fibroblasts stained immunocytochemically for α-SMA (red) and FN (green) and counterstained with DAPI (blue) after 3 days in culture with the treatments indicated in each image. Scale bars: 50 μm. Cont, control; T+15d-PGJ2, TGF-β plus15d-PGJ2; T+Rosi, TGF-β plus rosiglitazone; T+Trog, TGF-β plus troglitazone.

In contrast, at the same three day time-point, and as suggested by our earlier analysis of variance results, the three PPARγ ligands used here decreased levels of COL1 and FN to a similar extent and with no significant differences in apparent effectiveness between ligands. For COL1, they decreased expression from 11 ± 3-fold above baseline in the TGF-β1—only condition to approximately 2 ± 0.6-fold above baseline—about a fivefold reduction. For FN, PPARγ ligand treatment decreased its expression from approximately 25 ± 6-fold above baseline in the TGF-β1—only condition to approximately 5 ± 2.5-fold above baseline (also about a fivefold reduction).

Our observations can be summarized into four major findings: i) α-SMA appeared to be induced at greater relative levels than both COL1 and FN after exposure to TGF-β1, especially after 2 and 3 days in culture; ii) all three PPARγ ligands tested in the present experiments, whether electrophilic or nonelectrophilic, were able to decrease α-SMA induction at 2 and 3 days in culture; however, this occurred at different doses for the different compounds, and α-SMA levels returned to baseline only if the cultures were treated with either troglitazone or 15d-PGJ2 (not rosiglitazone); iii) all three ligands also decreased the induction of COL1 and FN in addition to α-SMA, but the levels of COL1 and FN remaining after treatment were still two- to fivefold above baseline, no matter which ligand was used; and iv) optimal doses of rosiglitazone and troglitazone were only able to reduce COL1 levels after 2 and 3 days of culture and FN levels only after 3 days in culture.

Antifibrotic Effects of PPARγ Ligands Are PPARγ Independent

Although PPARγ is widely expressed in the feline cornea, both in epithelial cells and stromal keratocytes (Supplemental Figure S1), it was important to test whether the observed antifibrotic effects of troglitazone, rosiglitazone, and 15d-PGJ2 in cultured feline corneal fibroblasts were PPARγ

dependent or independent. We first used a pharmacologic approach, co-incubating the optimal doses of the PPARγ ligands of interest with GW9662. In feline orbital fibroblasts, a cell type that can easily be induced to produce fat in a PPARγ-dependent manner,[29] GW9662 inhibited PPARγ ligand—induced fat production at doses ranging from 0.5 to 2 μmol/L, with 1 to 2 μmol/L proving equally and maximally effective (Supplemental Figure S2A). Although effective at reducing fat synthesis in cat orbital fibroblasts, 1 μmol/L GW9662 was unable to prevent the down-regulation of α-SMA, COL1, or FN expression induced by the three PPARγ ligands of interest in cultured cat corneal fibroblasts (Figure 5, A and B). In addition, 1 μmol/L GW9662 also did not influence TGF-β1—induced expression of α-SMA, COL1, and FN (Figure 5, A and B) in these cells, suggesting that the antifibrotic actions of the electrophilic and nonelectrophilic PPARγ ligands tested in feline corneal fibroblasts likely occurred via PPARγ-independent mechanisms.

We used a genetic approach as another method to test whether the antifibrotic actions of PPARγ ligands occur independently of PPARγ. PPARγ activity was blocked using a PPARγ-DN-Lv construct. The PPARγ-Lv construct expresses a mutant PPARγ (Flag tag-PPARγ1 L466A/E469A), which cannot activate transcription of PPARγ target genes and blocks activity of endogenous PPARγ.[31] To test whether PPARγ-DN could inhibit feline adipogenesis and thus feline PPARγ, GFP-Lv or PPARγ-DN-Lv were introduced into feline orbital fibroblasts by Lv infection. Infected cells were induced to differentiate into adipocytes with a standard adipogenic cocktail.[30] GFP-Lv—infected cells readily formed adipocytes, whereas PPARγ-DN-Lv—infected cells did not (Supplemental Figure S2B). These

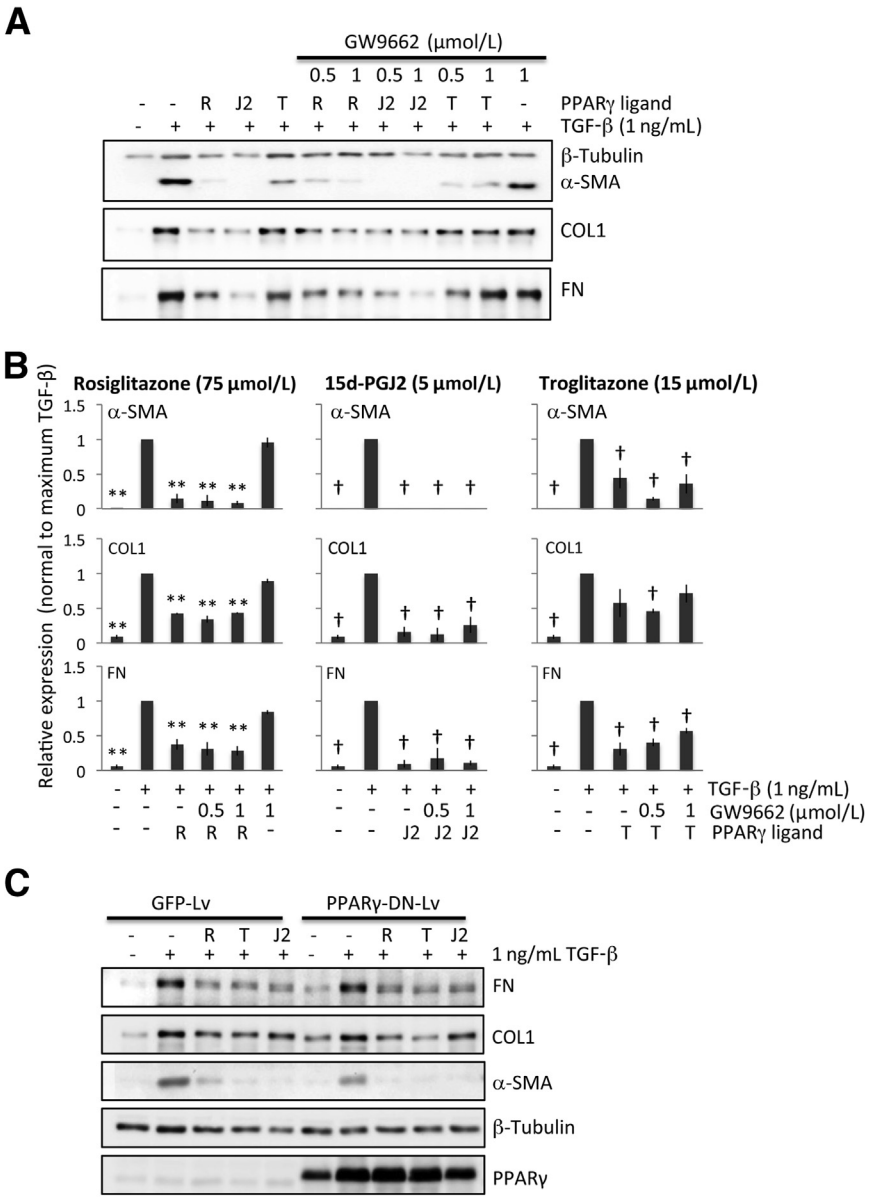

Figure 5 PPARγ dependence of antifibrotic effects exhibited by PPARγ ligands. **A:** Representative Western blots show protein levels for α-SMA, type 1 collagen (COL1), and fibronectin (FN). β-tubulin was used as a loading control. **B:** Plots of the relative expression of FN, COL1, and α-SMA normalized to the maximal densitometric values obtained in cells stimulated with 1 ng/mL of TGF-β1 for 3 culture days. Data are means ± SD averaged for three experiments. **C:** Western blot analysis of α-SMA, COL1, FN, β-tubulin (loading control), and PPARγ levels of GFP-Lv— or PPARγ-DN-Lv—infected corneal fibroblasts treated with vehicle, PPARγ ligands, and/or TGFβ. PPARγ-DN-Lv—infected corneal fibroblasts express high levels of flag-tagged PPARγ-DN protein (**upper band**) that blocks endogenous PPARγ (**lower band**) activity. $^{**}P < 0.01$ by Bonferroni-corrected Student's *t*-test for rosiglitazone relative to the TGF-β1—only condition; $^{\dagger}P < 0.0125$ by Bonferroni-corrected Student's *t*-test for troglitazone and 15d-PGJ2 relative to the TGF-β1—only condition in each graph ($df = 4$ for all tests).

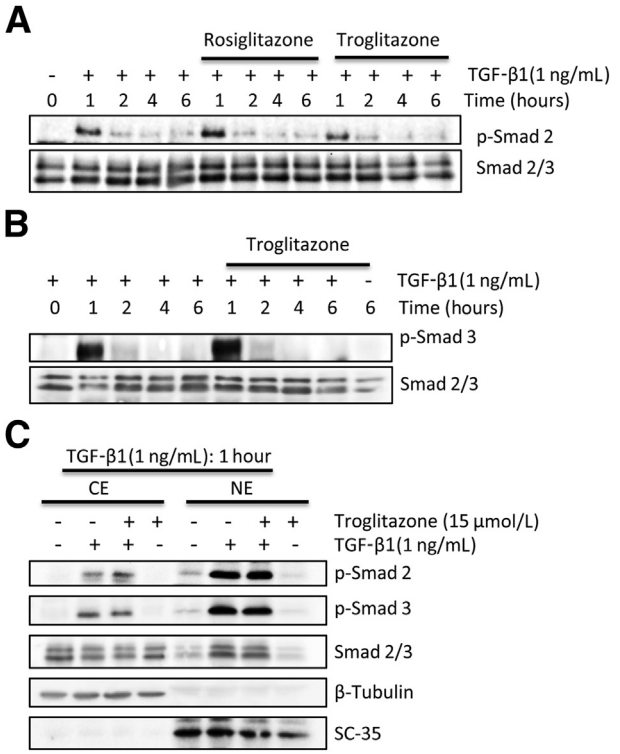

Figure 6 Effect of PPARγ ligands on TGF-β1—induced phosphorylation and nuclear translocation of Smads 2/3. **A:** Western blots show effect of rosiglitazone and troglitazone on TGF-β1—induced phosphorylation of Smad 2 protein. Total Smads 2/3 levels were assayed as a loading control. **B:** Preincubation with 15 μmol/L of troglitazone does not appear to inhibit TGF-β1—induced phosphorylation of Smad 3 or alter total levels of Smad 2/3. **C:** Western blots show the effect of troglitazone on TGF-β1—induced nuclear translocation of Smads 2/3. TGF-β1 increases the amount of phosphorylated Smads (p-Smad) 2 and 3 in both the nuclear (NE) and cytoplasmic (CE) fractions after the 1-hour incubation period (lanes 2 and 6). Preincubation with 15 μmol/L troglitazone before adding TGF-β1 does not alter the levels of p-Smads 2/3 or total Smads 2/3 in either fraction (lanes 3 and 7). Because TGF-β1 treatment moved p-Smads 2/3 into nucleus, the levels of total Smads 2/3 became uneven, with a smaller amount left in the cytoplasmic fraction (compare lanes 1 and 2) and a greater amount in the nucleus (compare lanes 5 and 6).

data revealed that PPARγ-DN could indeed inhibit feline PPARγ.

We then infected feline corneal fibroblasts with GFP or PPARγ-DN expressing Lv. Infected cells were treated with optimal doses of PPARγ ligands and TGF-β as described above, and cell extracts were analyzed for myofibroblast markers and PPARγ expression (Figure 5C). Expression of PPARγ-DN that blocks PPARγ activity had no effect on the ability of PPARγ ligands to inhibit expression of myofibroblast markers (α-SMA, COL1, and FN), confirming the pharmacologic results described above for GW9662 and strongly suggesting that the antifibrotic actions of PPARγ ligands likely occur independently of PPARγ.

PPARγ Ligands Do Not Affect TGF-β1—Induced Phosphorylation and Nuclear Translocation of Smads 2/3

Consistent with previous studies in other species,[32] exposure of cultured feline corneal fibroblasts to TGF-β1 for 1 hour resulted in a huge increase of phosphorylation of Smads 2 and 3 (Figure 6, A and B). Longer incubation times with TGF-β1 (up to 6 hours) saw levels of these phosphorylated proteins diminish relative to total Smads 2/3 (Figure 6, A and B). Preincubation with rosiglitazone and troglitazone (Figure 6A) failed to inhibit TGF-β1—induced phosphorylation of Smad 2 (Figure 6A) or Smad 3 for troglitazone (Figure 6B) at all of the time points examined. Total Smad 2/3 levels also remained unchanged (Figure 6, A and B).

Another key possible site of action of PPARγ ligands with respect to Smad signaling is translocation of phosphorylated Smads 2/3 to the nucleus. Thus, we assayed the relative amounts of phosphorylated Smads 2/3 in the cytoplasmic and nuclear fractions after a 1-hour incubation time with TGF-β1. TGF-β1 increased the amount of phosphorylated Smads 2 and 3 in both fractions after the 1-hour incubation period (Figure 6C). Pre-incubation of the cells with troglitazone before adding TGF-β1 did not alter the levels of phosphorylated Smads 2/3 or total Smads 2/3 in either fraction (Figure 6C). Finally, neither the vehicle (Figure 6C)

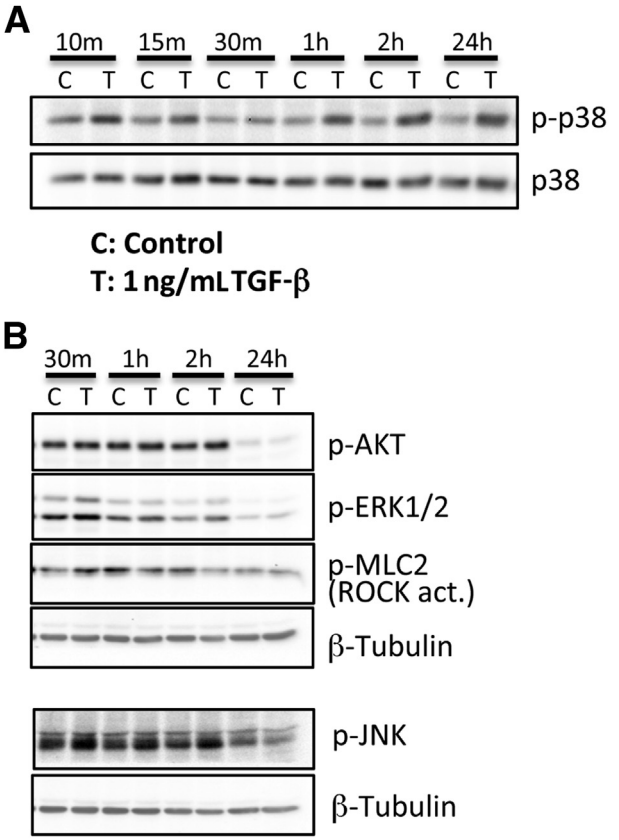

Figure 7 Effect of TGF-β1 stimulation on phosphorylation of non-Smad signaling molecules in cat corneal fibroblasts. Western blot shows the time course of control (C) and TGF-β stimulation (T) on the expression of phosphorylated p38 (p-p38) and total p38 (p38) in cultured cat corneal fibroblasts (**A**) and the effect of C and T on phosphorylated JNK (p-JNK), phosphorylated ERK1/2 (p-ERK1/2), phosphorylated AKT (p-AKT), and phosphorylated MLC2 (p-MLC2), with levels of β-tubulin assayed as a loading control (**B**). m, minutes; hr, hours

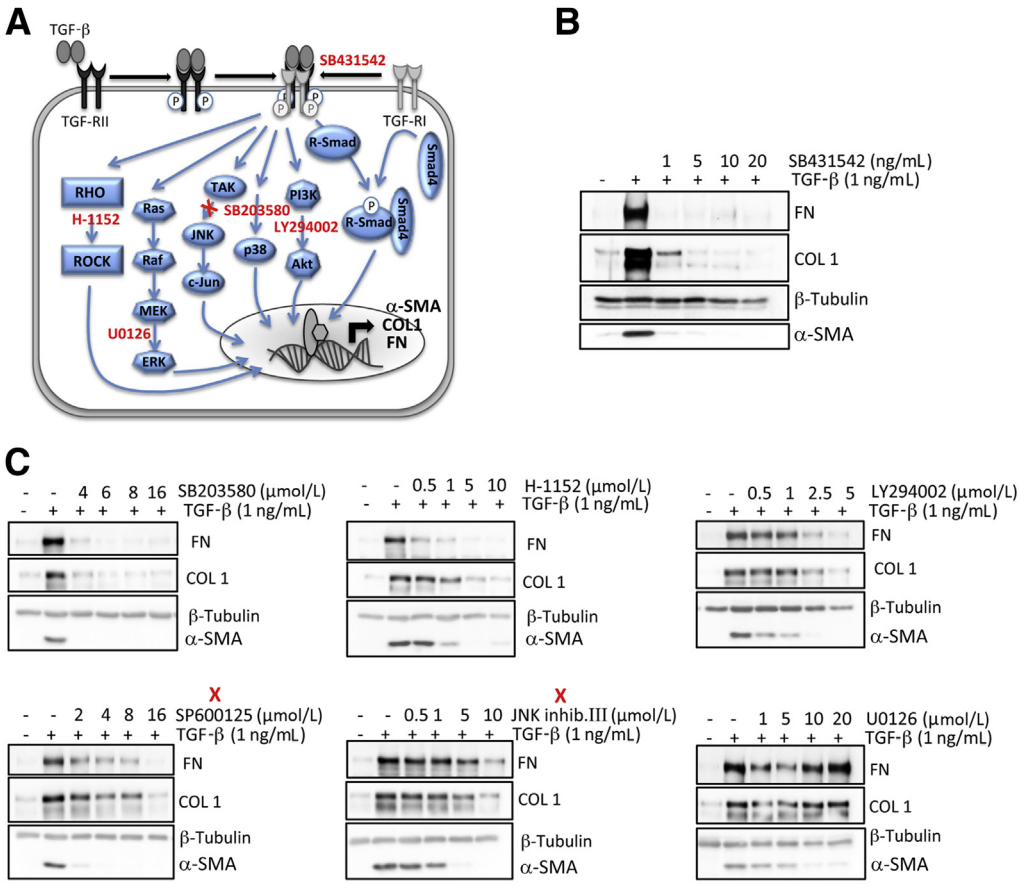

Figure 8 Effect of kinase inhibitors on TGF-β1—induced expression of α-SMA, collagen 1 (COL1), and fibronectin (FN). **A:** Model of the multiple signaling molecules and pathways activated by TGF-β binding to its receptor. The different kinase inhibitors used are indicated in red and positioned close to their putative site of action. **B:** Representative Western blots show the effect of the TGF-β receptor 1 inhibitor SB431542 (as a positive control) on TGF-β1—induced expression of α-SMA, COL1, and FN in cultured corneal fibroblasts. Used concentrations are indicated above each blot. **C:** Western blots showing effect of different inhibitors on TGF-β1—induced expression of α-SMA, COL1, and FN in cultured corneal fibroblasts. We used the Rho-kinase inhibitor H-1152, the ERK inhibitor U0126, the p38 inhibitor SB203580, the AKT inhibitor LY294002. **Red X**, indicates two different JNK inhibitors (SP600125 and JNK inhibitor III). Concentrations of each inhibitor used are shown above each blot.

nor troglitazone alone (Figure 6C) influenced phosphorylation of Smads 2/3 or their translocation into the nucleus. Thus, it seems that the antifibrotic actions of PPARγ ligands in corneal fibroblasts did not occur by blocking either TGF-β1—mediated phosphorylation or nuclear translocation of Smads 2/3 during the first 6 hours after treatment.

Effect of TGF-β1 Stimulation on Phosphorylation of Downstream Signaling Molecules

Accumulating evidence suggests that tetrameric TGF-β receptor complexes activate a number of Smad-independent signaling pathways, which may also play a role in generating fibrotic phenotypes in a range of body tissues.[9] Our goals were to identify which of these signaling pathways were most strongly activated by TGF-β in cat corneal fibroblasts under our particular cell culture conditions and to assess whether these pathways were influenced by optimal doses of PPARγ ligands, offering a possible substrate for their antifibrotic actions. We first assayed which of the main non-Smad signaling molecules were increased by incubation with TGF-β1 and over what time frame. As summarized in Figure 7A, the activation of p38 MAPK (in the form of increased levels of phosphorylated p38 relative to total p38) appeared to be the most significant change observed, starting within minutes after TGF-β1 stimulation and persisting for at least 24 hours. Phosphorylation of MLC2, indicative of ROCK activation, was also observed on incubation with TGF-β1 at 1 hour, but the effect disappeared thereafter (Figure 7B). In contrast, there were no TGF-β1—induced increases in levels of phosphorylated AKT, phosphorylated ERK1/2, and phosphorylated JNK compared with DMSO-treated vehicle at any of the time points examined (Figure 7B).

Effect of Kinase Inhibitors on TGF-β1—Induced Expression of α-SMA, COL1, and FN

To critically test whether phosphorylation of p38 was a key signal for translating TGF-β receptor binding into a myofibroblastic phenotype in corneal fibroblasts, we used small-molecule inhibitors (Figure 8A) to block endogenous

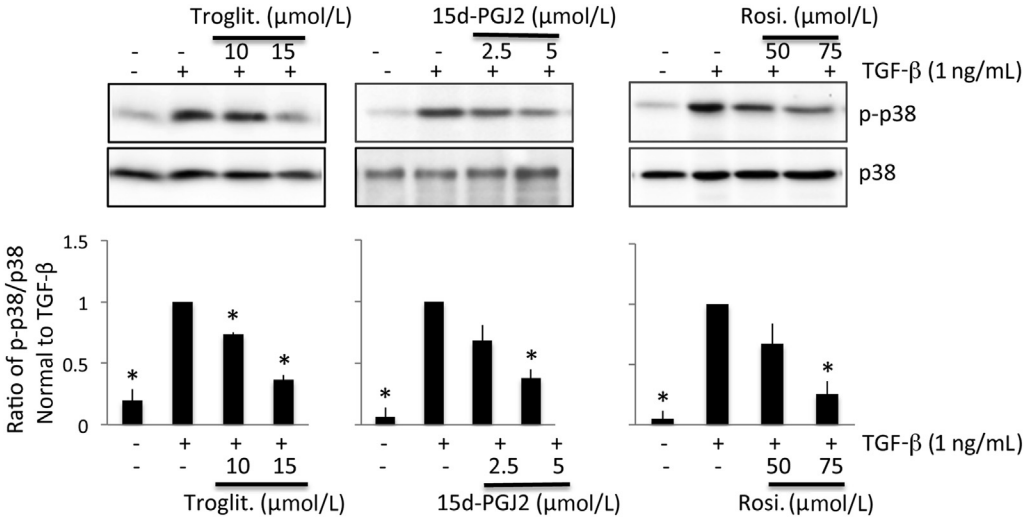

Figure 9 Effect of PPARγ ligands on TGF-β1–induced phosphorylation of p38 MAPK signaling in cultured corneal fibroblasts. Representative Western blots show the stimulatory effect of TGF-β1 on levels of phosphorylated p38 (p-p38) and the inhibitory actions of troglitazone (troglit.), 15d-PGJ2, and rosiglitazone (rosi.) on levels of p-p38. The three bar plots show the means ± SD of densitometric measures (specifically, the ratio of p-p38 to p38 for each treatment condition, normalized to the ratio obtained after TGF-β treatment alone) averaged for three separate experiments. $^*P < 0.0167$ by Bonferroni-corrected Student's *t*-test relative to the TGF-β1–only condition ($df = 4$ for all tests).

protein kinases responsible for phosphorylation in each of the signaling pathways examined earlier. We then assessed consequences of this inhibition on the expression of α-SMA, COL1, and FN after TGF-β1 stimulation. As expected, the TGF-β receptor 1 inhibitor (SB431542) eliminated TGF-β1–induced increases in α-SMA and FN expression at 1 ng/mL (Figure 8B); it also returned COL1 expression to basal levels at a slightly higher dose of 5 ng/mL (not shown). The other kinase inhibitors used also diminished α-SMA expression in a concentration-dependent manner (Figure 8C). The p38 kinase inhibitor (SB203580) and Rho-kinase inhibitor (H-1152) were almost as effective as the TGF-β receptor 1 inhibitor at concurrently blocking both the TGF-β1–induced increases in α-SMA, COL1, and FN expression, with a slight advantage exhibited by SB203580 at a dose of 4 to 5 μmol/L (Figure 8C). Other inhibitors (eg, the two JNK and the Akt kinase inhibitors) appeared to exert a stronger effect on α-SMA expression and a weaker effect on COL1 and FN expression (Figure 8C). The most extreme example of this was seen with the ERK kinase inhibitor, U0126 (Figure 8C), which prevented increases in α-SMA expression but failed to alter COL1 and FN expression, even at the highest dose (10 μmol/L) tested. Thus, in cat corneal fibroblasts, as in fibroblasts from other parts of the body, the tetrameric TGF-β receptor complex activated multiple intracellular pathways to induce the expression of profibrotic molecules. Although all of the pathways tested here influenced α-SMA expression to some extent, only a subset of these pathways also regulated expression of FN and COL1 at the same doses. Even for pathways that appeared to regulate COL1 and FN expression, higher doses of kinase inhibitors were usually required to exert the level of inhibition seen for α-SMA expression. The major exception was phosphorylation of p38 MAPK, whose inhibition appeared the most effective at blocking TGF-β1–induced increases in all three profibrotic molecules of interest at similar doses of the relevant kinase inhibitor.

PPARγ Ligands Decrease TGF-β1–Induced Phosphorylation of p38 MAPK

These experiments showed that among multiple signaling molecules that could mediate myofibroblast differentiation, p38 MAPK phosphorylation i) was reliably activated by TGF-β1 stimulation, ii) persisted for at least 24 hours after TGF-β1 stimulation, and iii) was inhibited by SB203580, which simultaneously prevented TGF-β1–induced increases in α-SMA, COL1, and FN expression. Our next question in this context was whether the PPARγ ligands of interest blocked TGF-β1–induced increases in α-SMA, COL1, and FN expression by decreasing phosphorylation of p38 MAPK in cultured corneal fibroblasts. As shown in Figure 9, troglitazone, rosiglitazone, and 15d-PGJ2 all decreased the levels of phosphorylated p38 MAPK induced by incubation with TGF-β1 in a dose-dependent manner. Importantly, the doses of these three drugs that were effective at decreasing levels of α-SMA, COL1, and FN expression (Figures 1, 2, and 3) were similarly effective at decreasing phosphorylated p38 MAPK expression (Figure 9). In contrast, total p38 MAPK levels were unaffected by addition of these three PPARγ ligands (Figure 9).

Troglitazone Is a Potent Antifibrotic during Corneal Wound Healing *in Vivo*

Finally, in an attempt to assess whether small molecule synthetic PPARγ ligands are able to curtail fibrosis after corneal wounding *in vivo*, we applied troglitazone topically

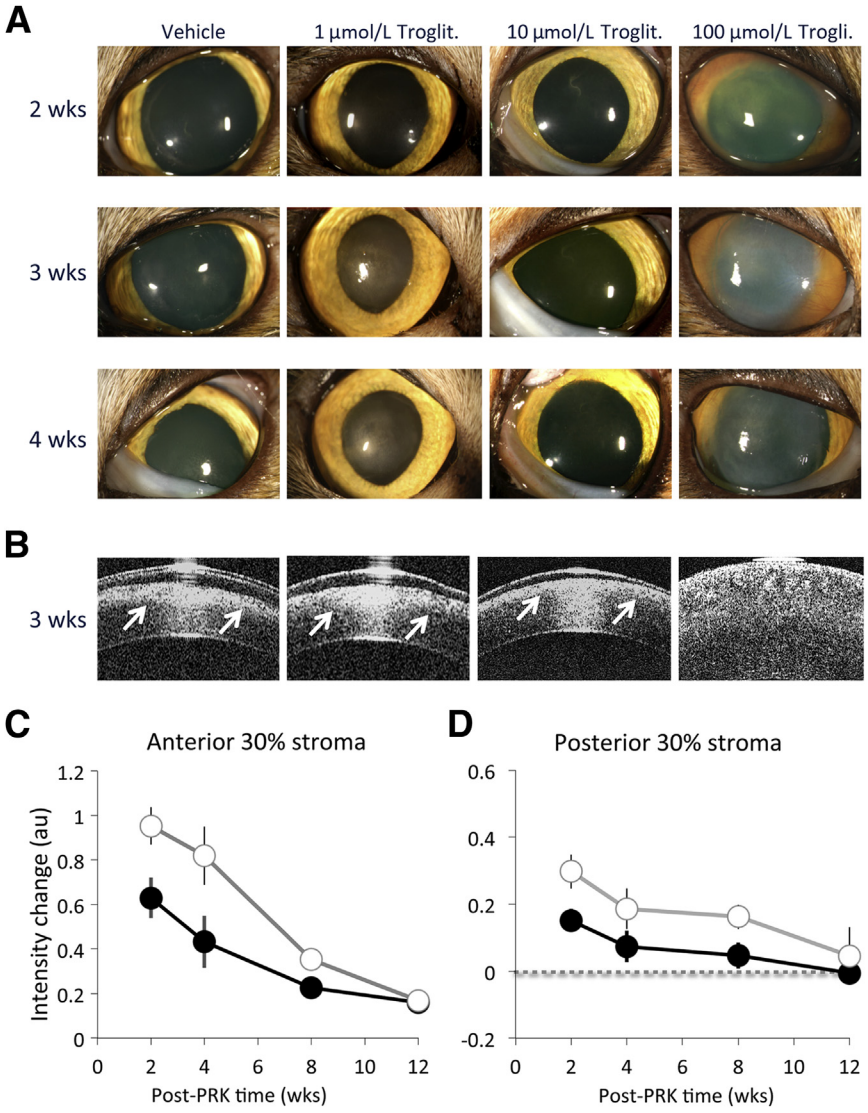

Figure 10 Antifibrotic effects of troglitazone *in vivo*. **A:** Photographs of four cat eyes who underwent conventional PRK with −10-Diopter ablation in a 6-mm optical zone. PRK was followed by topical application of either vehicle solution (10% DMSO in Celluvisc) or three different doses of troglitazone (troglit.) diluted in 10% DMSO/Celluvisc. Visual inspection of the cat eyes at different time points after PRK reveals a clear dose response in the effect of topical troglitazone relative to the vehicle solution. Note toxic reaction to 100 µmol/L troglitazone. **B:** OCT images of the cat eyes in **A** collected 3 weeks after operation. OCT imaging confirms the appearance of a band of increased stromal reflectivity at the ablation zone (**arrow**), which significantly decreases in eyes treated with 10 µmol/L troglitazone. **C:** Graphs of normalized intensity change in the anterior 30% of the stroma relative to preoperative values (zero), measured from OCT images such as those in **B**, and plotted separately for vehicle-treated (DMSO/Celluvisc) corneas (white symbols) or corneas that received 10 µmol/L troglitazone after PRK (black symbols). **D:** Graphs of normalized intensity change in the posterior 30% of the stroma relative to preoperative values (zero), measured from OCT images such as those in **B**, and plotted separately for vehicle-treated (DMSO/Celluvisc) corneas (white symbols) or corneas that received 10 µmol/L troglitazone after PRK (black symbols). Error bars indicate SEM (**C** and **D**). wks, weeks.

to live cat eyes after PRK. PRK involves epithelial debridement and laser ablation of the stromal bed to a depth of approximately 160 µm; it normally induces a strong wound healing reaction in the cat.[7,19,39] Visual inspection of the clarity of the cat corneas at different time points after PRK revealed a clear dose response in the effect of troglitazone relative to application of the vehicle solution alone (Figure 10A): 1 µmol/L troglitazone caused little reduction of haze relative to the application of vehicle solution after PRK. Application of 100 µmol/L troglitazone at the same rate caused overt corneal toxicity, evidenced by prolonged opacification and swelling of the cornea. Application of 10 µmol/L troglitazone resulted in better corneal clarity at early time points after PRK relative to vehicle-treated eyes. These findings were verified by OCT imaging (Figure 10, B–D) and histologic analysis (Figure 11). OCT imaging confirmed the appearance of a band of increased reflectivity occurring at the stromal ablation zone (Figure 10B). This band was thickest (ie, extending to the greatest depth into the cornea) in eyes receiving vehicle solution and 1 µmol/L troglitazone after PRK. The band of increased reflectivity was thinnest in the eyes treated with 10 µmol/L troglitazone after PRK. Eyes treated with 100 µmol/L troglitazone exhibited a pathologic corneal appearance on OCT, with significant swelling, increased reflectivity throughout the entire depth of the cornea, and the inability to clearly define an epithelial layer (Figure 10B).

At 2 weeks after PRK, quantitative analysis of OCT images in 10 cats showed that the backscatter reflectivity of the anterior 30% of the stroma of vehicle-treated eyes was increased by means ± SEM of 61% ± 5% relative to preoperative levels. In contrast, eyes treated with 10 µmol/L troglitazone exhibited an increase of only 39% ± 6% at the end of treatment, a statistically significant difference ($P = 0.0149$, Student's t-test, $df = 18$). By 4 weeks after PRK, 2 weeks after the end of treatment, backscatter reflectivity of the anterior 30% of the stroma was still 52% ± 8% higher than preoperatively in vehicle-treated eyes. In troglitazone-treated

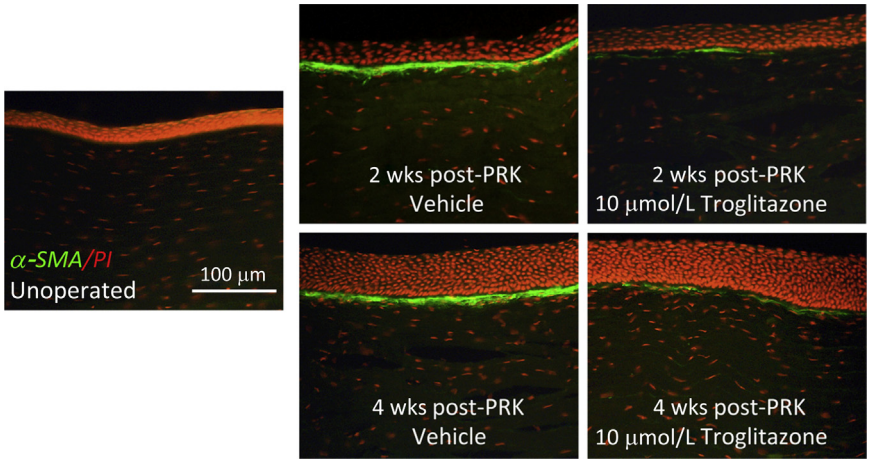

Figure 11 Immunostaining for α-SMA (green) in cat corneal sections counterstained with propidium iodide (PI-red) of postmortem cat corneas. No α-SMA staining is observed in unoperated on corneas. Note the strongly stained, continuous band of α-SMA—positive cells in the stroma adjacent to the ablation zone at both 2 and 4 weeks after PRK in vehicle-treated eyes. In contrast, there is a significant reduction in α-SMA expression in the corneas treated with 10 μm troglitazone and examined at both 2 and 4 weeks after PRK.

eyes, this value was approximately half, at 27% ± 7%, also a statistically significant difference ($P = 0.043$, Student's *t*-test, $df = 14$). By 12 weeks postoperatively, backscatter reflectivity in vehicle-treated eyes was only 11% ± 2.5% greater than preoperative levels, whereas in troglitazone-treated eyes, it was 10% ± 3.0% greater, values that were no longer significantly different from each other (Figure 10C). A two-way analysis of variance was conducted to examine the effect of postoperative treatment (10 μmol/L troglitazone or vehicle) and time (2, 4, 8, and 12 weeks after PRK) on change in backscatter reflectivity in the anterior 30% of the stroma. There were significant main effects of treatment ($F_{1,44} = 6.605$, $P = 0.014$) and time ($F_{3,44} = 14.891$, $P < 0.0005$) on reflectivity but no significant interaction between the two ($F_{3,44} = 1.235$, $P = 0.308$). A similar result was obtained for backscatter reflectivity in the posterior 30% of the stroma (Figure 10D). There was a significant main effect of treatment ($F_{1,44} = 6.562$, $P = 0.014$) and time ($F_{3,44} = 4.442$, $P = 0.008$) on reflectivity but no significant interaction between the two ($F_{3,44} = 0.225$, $P = 0.878$). The posterior stromal reflectivity was increased significantly above preoperative levels up to 8 weeks after PRK in vehicle-treated eyes (Figure 10D). In contrast, troglitazone-treated eyes (Figure 10D) exhibited half the increase seen in vehicle-treated eyes at 2 weeks after PRK, and by 4 weeks after PRK, intensity levels had decreased enough that they were no longer significantly higher than preoperatively.

Immunofluorescent staining of corneas from the different treatment groups post mortem revealed a strongly stained, continuous band of α-SMA—positive cells in the anterior stroma of the ablation zone at both 2 and 4 weeks after PRK in vehicle-treated eyes (Figure 11). In contrast, 10 μmol/L of troglitazone applied topically every day for 2 weeks postoperatively significantly inhibited the development of this α-SMA—positive zone at both 2 and 4 weeks after PRK. Only a few, dispersed clusters of α-SMA—positive cells were seen under the epithelium at both time points (Figure 11). This result indicates that the antifibrotic actions of PPARγ ligands reported above in cultured feline corneal fibroblasts also apply *in vivo*, when such compounds are used topically in live cat eyes after corneal wounding.

Discussion

Corneal scarring is a predominant affliction worldwide. It has no effective treatment without adverse effects and when untreated can cause blindness.[42] Finding a safe way of controlling corneal scarring and fibrosis would be of tremendous public health benefit.

Recently, we reported on the beneficial optical and biological consequences of using rosiglitazone, a synthetic PPARγ ligand, topically in cat eyes to control fibrosis after PRK.[19] However, we do not know how rosiglitazone exerts its antifibrotic actions in the cornea or whether it is unique among PPARγ ligands in being able to act this way. Moreover, the successful application of rosiglitazone to treat corneal fibrosis *in vivo* seemed to run counter to its weak effects in a prior *in vitro* study using human corneal fibroblasts.[16] Thus, we characterized the mechanisms of antifibrotic action of rosiglitazone and two other PPARγ ligands in feline corneal fibroblasts *in vitro*. We found these cells to behave similarly in culture compared with corneal fibroblasts from rabbits,[43] cows,[25] and humans.[44]

TGF-β1 stimulation caused cat corneal fibroblasts to express α-SMA, COL1, and FN at increasing levels during consecutive days, just as it did in corneal fibroblasts from other species.[25,43,44] Both electrophilic (15d-PGJ2) and nonelectrophilic (rosiglitazone and troglitazone) PPARγ ligands almost completely blocked the TGF-β—induced increases in α-SMA expression. These drugs also significantly reduced increases in the intracellular expression of COL1 and FN, although never back to baseline levels. Notably, the doses of 15d-PGJ2 needed to exert these effects (2.5 to 5 μmol/L) were much lower than the doses of troglitazone (10 to 15 μmol/L) and rosiglitazone (50 to 75 μmol/L). Thus, our results confirm and may even explain data from prior *in vitro* studies that reported lack of effectiveness of rosiglitazone in

human corneal fibroblasts but only used this drug at a maximal dose of 10 μmol/L.[16] We found this dose to be relatively ineffective at decreasing myofibroblast transformation in cat corneal cells.

Prior work in a variety of tissues suggested that the antifibrotic actions of PPARγ ligands occurred via a combination of PPARγ-dependent and -independent mechanisms.[23,45,46] In cultured rabbit corneal fibroblasts, Pan et al[18] came to the same conclusion with respect to pioglitazone's antifibrotic actions. However, in human corneal fibroblasts, Kuriyan et al[16] found that the antifibrotic effects of CDDO-Me and 15d-PGJ2 were largely PPARγ independent. In the present experiments, we used both a pharmacologic[47] and a DN genetic approach[16,31] to block PPARγ *in vitro*. We first verified that in feline orbital fibroblasts, as in those from other species,[48] PPARγ ligands were able to increase fat production in a PPARγ-dependent manner. We then found that neither pharmacologic nor genetic blockade of PPARγ function were able to prevent, even partially, the antifibrotic effects of the three PPARγ ligands of interest in cat corneal fibroblasts. Why our findings differ from those of Pan et al[18] remains a matter of speculation. Differences in cell culture conditions, treatment times (3 days in the present study versus 1 day in theirs), and the mechanisms of action of pioglitazone versus the PPARγ ligands tested here are among the possible explanations.

If PPARγ ligands did not work via PPARγ, a reasonable next question was whether they might control corneal fibrosis by regulating Smads 2/3. As expected, we found that TGF-β1 increased the phosphorylation and nuclear translocation of Smads 2/3 in cat corneal fibroblasts. However, optimal doses of our PPARγ ligands of interest did not seem to influence either process, prompting us to probe some of the other signaling pathways activated by TGF-β stimulation, including ERK1/2, p38 MAPK, JNK MAPK, Rho, and AKT.[9] We used small-molecule inhibitors to block key protein kinases responsible for phosphorylation in each pathway and assessed whether these inhibitors prevented TGF-β1–induced increases in the expression of α-SMA, COL1, and FN. We observed i) equivalent blockage of α-SMA, COL1, and FN expression (H-1152, SB203580, and SB431542); ii) a stronger block on α-SMA and a weaker block on COL1 and FN expression (SP600125, JNK inhibitor III, LY294002); or iii) blockage of α-SMA but no effect on COL1 and FN expression (U0126). Thus, the signaling molecules downstream of TGF-β receptor activation appeared to differentially regulate synthesis of α-SMA versus extracellular matrix components in corneal fibroblasts. However, p38 MAPK was the only molecule i) whose phosphorylation was reliably induced by TGF-β1 stimulation, ii) for which the TGF-β1–related induction persisted for at least 24 hours, and iii) whose inhibition with SB203580 simultaneously prevented TGF-β1–induced increases in α-SMA, COL1, and FN expression. Huh et al[49] also reported that p38 MAPK was an important TGF-β–induced intermediate in corneal fibrotic wound repair and that it co-localized with α-SMA *in vivo*. More recently, Yang et al[50] reported that among MAPKs, p38 MAPK activation by TGF-β was critical to sustain activation of Smad 2 for an extended period. This, in turn, was necessary for myofibroblast differentiation.

A final piece of supporting evidence for the putative role of p38 MAPK in mediating the antifibrotic actions of PPARγ ligands in cultured, cat corneal fibroblasts was that doses of 15d-PGJ2, troglitazone, and rosiglitazone that were optimal for blocking induction of α-SMA, COL1, and FN also blocked the TGF-β–induced increase in phosphorylated p38 MAPK. In view of the work of Yang et al,[50] we hypothesize that PPARγ ligands, by blocking TGF-β–induced p38 MAPK activation, should decrease Smad 2 activation at *late* time points rather than the early time points (Figure 6) after TGF-β stimulation.

With respect to *in vivo* testing, application of troglitazone to the ocular surface after PRK decreased stromal α-SMA expression at 2 and 4 weeks postoperatively, consistent with our previous results with rosiglitazone in this animal model.[19] OCT imaging at these time points revealed troglitazone to also decrease the size and intensity of the band of high backscatter reflectivity normally induced by PRK in the ablation zone stroma. There was a clear dose response for the effects of troglitazone in cat eyes, with doses 10× lower than the optimal exerting little visible effect and doses 10× higher than the optimal exerting a toxic effect. The cause of the toxicity remains to be determined, but we posit that it may involve endothelial failure, which would explain the observed corneal swelling and opacification. In summary, rosiglitazone is not unique among PPARγ ligands for exerting antifibrotic effects in the cornea *in vivo*. Troglitazone exerts a similar effect, and it is likely that other PPARγ ligands may also be good candidates as antiscarring medications for the cornea. However, given their different effective doses *in vitro* and the significant consequences of toxicity in the cornea, it seems prudent that careful dose-response determinations be made separately for each drug *in vivo*.

In conclusion, the present results reveal several different PPARγ ligands to be effective corneal antifibrotics *in vitro* and *in vivo*. Electrophilic ligands appear to be more effective at lower doses than nonelectrophilic ligands. All three PPARγ ligands tested appeared to function via PPARγ- and early Smad 2/3–independent signaling. Instead, they altered phosphorylation of p38 MAPK. Future studies should elucidate downstream and upstream components of the p38 pathway affected by PPARγ ligands and the effect of these small molecules on the other critical, cellular components of the cornea—the epithelial and endothelial cell layers. Nevertheless, our findings suggest that PPARγ ligands may be a promising class of antifibrotic drugs for corneal applications.

Acknowledgments

We thank Thurma McDaniel for performing immunostaining, Margaret DeMagistris for excellent technical assistance

with *in vivo* cat experiments, Tracy Bubel for tissue processing of cat eyes after PRK, and Dr. Larry W. Fisher (NIH, Bethesda, MD) for providing the anti-COL1 antibody.

Supplemental Data

Supplemental material for this article can be found at *http://dx.doi.org/10.1016/j.ajpath.2014.01.026*.

References

1. Jester JV, Barry-Lane PA, Cavanagh HD, Petroll WM: Induction of alpha-smooth muscle actin expression and myofibroblast transformation in cultured corneal keratocytes. Cornea 1996, 15:505–516
2. Vesaluoma M, Teppo AM, Gronhagen-Riska C, Tervo T: Release of TGF-beta 1 and VEGF in tears following photorefractive keratectomy. Curr Eye Res 1997, 16:19–25
3. Fini ME: Keratocyte and fibroblast phenotypes in the repairing cornea. Prog Retin Eye Res 1999, 18:529–551
4. Jester JV, Rodrigues MM, Herman IM: Characterization of avascular corneal wound healing fibroblasts. New insights into the myofibroblast. Am J Pathol 1987, 127:140–148
5. Wilson SE: Corneal myofibroblast biology and pathobiology: generation, persistence, and transparency. Exp Eye Res 2012, 99:78–88
6. Hinz B: The myofibroblast: paradigm for a mechanically active cell. J Biomech 2010, 43:146–155
7. Buhren J, Nagy L, Swanton JN, Kenner S, MacRae S, Phipps RP, Huxlin KR: Optical effects of anti-TGFβ treatment after photorefractive keratectomy in a cat model. Invest Ophthalmol Vis Sci 2009, 50:634–643
8. Kang JS, Liu C, Derynck R: New regulatory mechanisms of TGF-β receptor function. Trends Cell Biol 2009, 19:385–394
9. Mu Y, Gudey SK, Landstrom M: Non-Smad signaling pathways. Cell Tissue Res 2012, 347:11–20
10. Ikushima H, Miyazono K: TGFβ signalling: a complex web in cancer progression. Nat Rev Cancer 2010, 10:415–424
11. Moller-Pedersen T, Cavanagh HD, Petroll WM, Jester JV: Neutralizing antibody to TGFβ modulates stromal fibrosis but not regression of photoablative effect following PRK. Curr Eye Res 1998, 17:736–747
12. Santhiago MR, Netto MV, Wilson SE: Mitomycin C: biological effects and use in refractive surgery. Cornea 2012, 31:311–321
13. Talamo JH, Gollamudi S, Green WR, De La Cruz Z, Filatov V, Stark WJ: Modulation of corneal wound healing after excimer laser keratomileusis using topical mitomycin C and steroids. Arch Ophthalmol 1991, 109:1141–1146
14. Jester JV, Nien CJ, Vasiliou V, Brown DJ: Quiescent keratocytes fail to repair MMC induced DNA damage leading to the long-term inhibition of myofibroblast differentiation and wound healing. Mol Vision 2012, 18:1828–1839
15. Erdurmus M, Cohen EJ, Yildiz EH, Hammersmith KM, Laibson PR, Varssano D, Rapuano CJ: Steroid-induced intraocular pressure elevation or glaucoma after penetrating keratoplasty in patients with keratoconus or Fuchs dystrophy. Cornea 2009, 28:759–764
16. Kuriyan AE, Lehmann GM, Kulkarni AA, Woeller CF, Feldon SE, Hindman HB, Sime PJ, Huxlin KR, Phipps RP: Electrophilic PPARγ ligands inhibit corneal fibroblast to myofibroblast differentiation in vitro: a potentially novel therapy for corneal scarring. Exp Eye Res 2012, 94:136–145
17. Pan H, Chen J, Xu J, Chen M, Ma R: Antifibrotic effect by activation of peroxisome proliferator-activated receptor-gamma in corneal fibroblasts. Mol Vis 2009, 15:2279–2286
18. Pan HW, Xu JT, Chen JS: Pioglitazone inhibits TGFβ induced keratocyte transformation to myofibroblast and extracellular matrix production. Mol Biol Rep 2011, 38:4501–4508
19. Huxlin KR, Hindman HB, Jeon KI, Buhren J, MacRae S, DeMagistris M, Ciufo D, Sime PJ, Phipps RP: Topical rosiglitazone is an effective anti-scarring agent in the cornea. PLoS One 2013, 8:e70785
20. Simpson-Haidaris PJ, Pollock SJ, Ramon S, Guo N, Woeller CF, Feldon SE, Phipps RP: Anticancer role of PPARγ agonists in hematological malignancies found in the vasculature, marrow, and eyes. PPAR Res 2010, 2010:814609
21. Zhou B, Buckley ST, Patel V, Liu Y, Luo J, Krishnaveni MS, Ivan M, DeMaio L, Kim KJ, Ehrhardt C, Crandall ED, Borok Z: Troglitazone attenuates TGF-β1-induced EMT in alveolar epithelial cells via a PPARγ-independent mechanism. PLoS One 2012, 7:e38827
22. Ghosh AK, Bhattacharyya S, Lakos G, Chen SJ, Mori Y, Varga J: Disruption of transforming growth factor beta signaling and profibrotic responses in normal skin fibroblasts by peroxisome proliferator-activated receptor gamma. Arthritis Rheum 2004, 50:1305–1318
23. Liu Y, Dai B, Xu C, Fu L, Hua Z, Mei C: Rosiglitazone inhibits transforming growth factor-beta1 mediated fibrogenesis in ADPKD cyst-lining epithelial cells. PLoS One 2011, 6:e28915
24. Funderburgh JL, Funderburgh ML, Mann MM, Prakash S, Conrad GW: Synthesis of corneal keratan sulfate proteoglycans by bovine keratocytes in vitro. J Biol Chem 1996, 271:31431–31436
25. Beales MP, Funderburgh JL, Jester JV, Hassell JR: Proteoglycan synthesis by bovine keratocytes and corneal fibroblasts: maintenance of the keratocyte phenotype in culture. Invest Ophthalmol Vis Sci 1999, 40:1658–1663
26. Chen YH, Wang IJ, Young TH: Formation of keratocyte spheroids on chitosan-coated surface can maintain keratocyte phenotypes. Tissue Eng Part A 2009, 15:2001–2013
27. Oida T, Weiner HL: Depletion of TGF-β from fetal bovine serum. J Immunol Methods 2010, 362:195–198
28. Munger JS, Harpel JG, Gleizes PE, Mazzieri R, Nunes I, Rifkin DB: Latent transforming growth factor-β: structural features and mechanisms of activation. Kidney Int 1997, 51:1376–1382
29. Forman BM, Tontonoz P, Chen J, Brun RP, Spiegelman BM, Evans RM: 15-Deoxy-Δ 12, 14-prostaglandin J2 is a ligand for the adipocyte determination factor PPARγ. Cell 1995, 83:803–812
30. Hauner H, Skurk T, Wabitsch M: Cultures of human adipose precursor cells. Methods Mol Biol 2001, 155:239–247
31. Garcia-Bates TM, Bernstein SH, Phipps RP: Peroxisome proliferator-activated receptor gamma overexpression suppresses growth and induces apoptosis in human multiple myeloma cells. Clin Cancer Res 2008, 14:6414–6425
32. Inman GJ, Nicolas FJ, Hill CS: Nucleocytoplasmic shuttling of Smads 2, 3, and 4 permits sensing of TGF-beta receptor activity. Mol Cell 2002, 10:283–294
33. Inman GJ, Nicolas FJ, Callahan JF, Harling JD, Gaster LM, Reith AD, Laping NJ, Hill CS: SB-431542 is a potent and specific inhibitor of transforming growth factor-β superfamily type I activin receptor-like kinase (ALK) receptors ALK4, ALK5, and ALK7. Mol Pharmacol 2002, 62:65–74
34. Tura A, Grisanti S, Petermeier K, Henke-Fahle S: The Rho-kinase inhibitor H-1152P suppresses the wound-healing activities of human Tenon's capsule fibroblasts in vitro. Invest Ophthalmol Vis Sci 2007, 48:2152–2161
35. Marampon F, Gravina GL, Di Rocco A, Bonfili P, Di Staso M, Fardella C, Polidoro L, Ciccarelli C, Festuccia C, Popov VM, Pestell RG, Tombolini V, Zani BM: MEK/ERK inhibitor U0126 increases the radiosensitivity of rhabdomyosarcoma cells in vitro and in vivo by downregulating growth and DNA repair signals. Mol Cancer Ther 2011, 10:159–168
36. Wang Y, Ji HX, Xing SH, Pei DS, Guan QH: SP600125, a selective JNK inhibitor, protects ischemic renal injury via suppressing the extrinsic pathways of apoptosis. Life Sci 2007, 80:2067–2075
37. Barancik M, Bohacova V, Kvackajova J, Hudecova S, Krizanova O, Breier A: SB203580, a specific inhibitor of p38-MAPK pathway, is a new reversal agent of P-glycoprotein-mediated multidrug resistance. Eur J Pharm Sci 2001, 14:29–36

38. Gharbi SI, Zvelebil MJ, Shuttleworth SJ, Hancox T, Saghir N, Timms JF, Waterfield MD: Exploring the specificity of the PI3K family inhibitor LY294002. Biochem J 2007, 404:15–21
39. Nagy LJ, MacRae S, Yoon G, Wyble M, Wang J, Cox I, Huxlin KR: Photorefractive keratectomy in the cat eye: biological and optical outcomes. J Cataract Refract Surg 2007, 33:1051–1064
40. Wang J, Thomas J, Cox I: Corneal light backscatter measured by optical coherence tomography after LASIK. J Refract Surg 2006, 22:604–610
41. Mukherjee R, Jow L, Croston GE, Paterniti JR Jr: Identification, characterization, and tissue distribution of human peroxisome proliferator-activated receptor (PPAR) isoforms PPARγ2 versus PPARγ1 and activation with retinoid X receptor agonists and antagonists. J Biol Chem 1997, 272:8071–8076
42. Whitcher JP, Srinivasan M, Upadhyay MP: Corneal blindness: a global perspective. Bull World Health Organ 2001, 79:214–221
43. Jester JV, Huang J, Barry-Lane PA, Kao WW, Petroll WM, Cavanagh HD: Transforming growth factor β-mediated corneal myofibroblast differentiation requires actin and fibronectin assembly. Invest Ophthalmol Vis Sci 1999, 40:1959–1967
44. Pei Y, Sherry DM, McDermott AM: Thy-1 distinguishes human corneal fibroblasts and myofibroblasts from keratocytes. Exp Eye Res 2004, 79:705–712
45. Ferguson HE, Kulkarni A, Lehmann GM, Garcia-Bates TM, Thatcher TH, Huxlin KR, Phipps RP, Sime PJ: Electrophilic peroxisome proliferator-activated receptor-gamma ligands have potent antifibrotic effects in human lung fibroblasts. Am J Respir Cell Mol Biol 2009, 41:722–730
46. Kulkarni AA, Thatcher TH, Olsen KC, Maggirwar SB, Phipps RP, Sime PJ: PPAR-gamma ligands repress TGFβ-induced myofibroblast differentiation by targeting the PI3K/Akt pathway: implications for therapy of fibrosis. PLoS One 2011, 6:e15909
47. Leesnitzer LM, Parks DJ, Bledsoe RK, Cobb JE, Collins JL, Consler TG, Davis RG, Hull-Ryde EA, Lenhard JM, Patel L, Plunket KD, Shenk JL, Stimmel JB, Therapontos C, Willson TM, Blanchard SG: Functional consequences of cysteine modification in the ligand binding sites of peroxisome proliferator activated receptors by GW9662. Biochemistry 2002, 41:6640–6650
48. Feldon SE, O'Loughlin CW, Ray DM, Landskroner-Eiger S, Seweryniak KE, Phipps RP: Activated human T lymphocytes express cyclooxygenase-2 and produce proadipogenic prostaglandins that drive human orbital fibroblast differentiation to adipocytes. Am J Pathol 2006, 169:1183–1193
49. Huh MI, Kim YH, Park JH, Bae SW, Kim MH, Chang Y, Kim SJ, Lee SR, Lee YS, Jin EJ, Sonn JK, Kang SS, Jung JC: Distribution of TGF-β isoforms and signaling intermediates in corneal fibrotic wound repair. J Cell Biochem 2009, 108:476–488
50. Yang Y, Wang Z, Yang H, Wang L, Gillespie SR, Wolosin JM, Bernstein AM, Reinach PS: TRPV1 potentiates TGFβ-induction of corneal myofibroblast development through an oxidative stress-mediated p38-SMAD2 signaling loop. PLoS One 2013, 8:e77300